Enzymes are often compartmentalized (stored in a specific part of the cell where they do their job) – for instance, in a particular organelle such as the membrane-based lysosomes. Compartmentalization means that enzymes needed for specific processes can be kept in the places where they act, ensuring they can find their substrates readily, don't damage the cell, and have the right microenvironment to work well. For instance, digestive enzymes of the lysosome work best at a pH around 5.0, which is found in the acidic interior of the lysosome (but not in the cytosol, which has a pH of about 7.2). Lysosomal enzymes have low activity at the pH of the cytosol, which may serve as "insurance" for the cell: even if a lysosome bursts and spills its enzymes, the enzymes will not begin digesting the cell, because they will no longer have the right pH to function. Some enzymes require the addition of another non-protein molecule to function. These "helper molecules" that assist in biochemical transformations are known as co-factors. Co-factors can be divided into two types, inorganic ions (e.g., zinc ions) referred to as catalysts and complex organic molecules (e.g., ATP [for phosphate group transfer], NADPH [for transfer of hydridion, i.e., 2 electrons and H^+], UDPGA [for the transfer of the glucuronosyl group] or UDP-glucose [for glucose transfer]) called co-enzymes. Co-enzymes are mostly derived from vitamins and other organic essential nutrients in small amounts. Co-enzymes are further divided into two types. The first is called a "prosthetic group," which consists of a co-enzyme that is tightly or even covalently, and therefore permanently bound to a protein. The second type of co-enzymes are called "co-substrates," which are transiently bound to the protein. Co-substrates may be released from a protein at some point and then rebind later. An inactive enzyme without the co-factor is called an apoenzyme, while the complete enzyme with co-factor is called a holoenzyme. Classification of enzymes (and transporters) depends on the extent of amino acid sequence identity. Enzymes with less than 40% amino acid sequence identity are assigned to different gene families (e.g., CYP1 and CYP2). Subfamilies comprise enzymes with 40–55% amino acid sequence identity (e.g., CYP2A and CYP2B), whereas isoforms denote enzymes with more than 55% amino acid identity (e.g., CYP3A4 and CYP3A5).

The time vs. concentration curves for the loss of substrate and the production of product during an enzyme-catalyzed reaction typically exhibit first-order relationships, as illustrated in Figure 1.14.

Because enzymes are not consumed by the reactions they catalyze (i.e., in its most naive interpretation, one assumes the free enzyme concentration $C(E)$ to be constant), metabolism is considered to be a very simple chemical (first-order) reaction in which a molecule S decomposes irreversibly to a product M. At the start of the reaction, we have some finite amount of S, symbolized by $C(S)_0$. At any time later, the amount of S remaining will be less than $C(S)_0$ and is symbolized with $C(S)_t$. The amount of S will decline with time until there is no S left, at which point the reaction will stop. Hence, in accordance with the relationships discussed in Section 1.1,

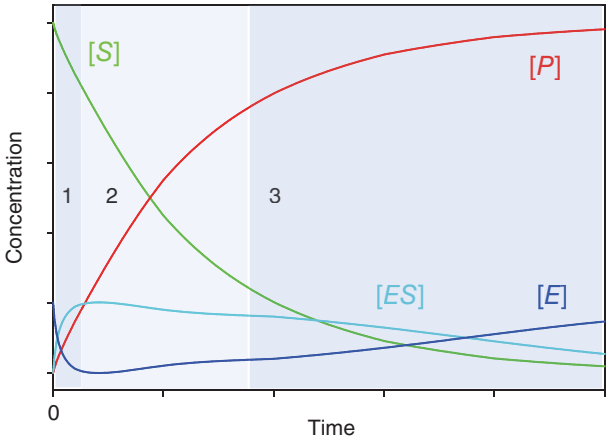


Figure 1.14 Time-dependent concentrations change (i.e., so-called reaction progress curves) for the multiple reaction partners involved in an enzyme-catalyzed reaction. Source: Adapted from Bisswanger [6]. Note that the substrate depletion curve (green line) is the mirror image of the product appearance (red line) curve (compare Figure 1.2). At early times, substrate loss and product appearance change rapidly with time, but as time increases, these rates diminish, reaching zero when all the substrate has been converted to product by enzyme: (i) pre-steady-state phase, (ii) pseudo steady-state phase, and (3) post-steady-state phase following substrate depletion. *S* = substrate, *P* = product, *E* = free enzyme, and *ES* = enzyme-substrate complex.

we expect that the reaction rate will be proportional to the amount of S present as follows:

$$\overline{\vartheta} = -\frac{dC(S)}{dt} = \frac{dC(M)}{dt} = k_1 \cdot C(S)_t \cdot C(E) = k_1' \cdot C(S)_t \tag{1.91}$$

where k_1' is the (pseudo) first-order rate constant for the overall reaction. Following integration, one obtains (compare Equation 1.6):

$$C(S)_t = C(S)_0 \cdot e^{-k_1' \cdot t} \tag{1.92}$$

Combination of Equations 1.91 and 1.92 gives:

$$\overline{\vartheta} = -\frac{dC(S)}{dt} = k_1' \cdot C(S)_0 \cdot e^{-k_1' \cdot t} \tag{1.93}$$

Equation 1.92 indicates that substrate concentration will decay exponentially from $C(S)_t = C(S)_0$ at $t = 0$ to $C(S)_t = 0$ at infinite time. Over this time period, the product concentration grows exponentially.

Factors Affecting the Velocity of Enzymatic Reactions!

The velocity of an enzymatic reaction can display, independent of the substrate concentration, remarkable sensitivity to a number of solution conditions. Failure to control these parameters can lead to significant errors or lack of reproducibility in experimental velocity measurements. The most important parameters to control are [5]:

Temperature: It is often observed that increasing the temperature of a chemical reaction by 10 °C roughly doubles its rate. Enzymes, like most chemical catalysts, show greater activity as temperature rises. However, because enzymes are also proteins, they become susceptible to thermal denaturation at higher temperatures. As a result, the boost in catalytic efficiency gained from increasing temperature is counterbalanced by the loss of activity caused by protein unfolding at elevated temperatures (Figure 1.15).

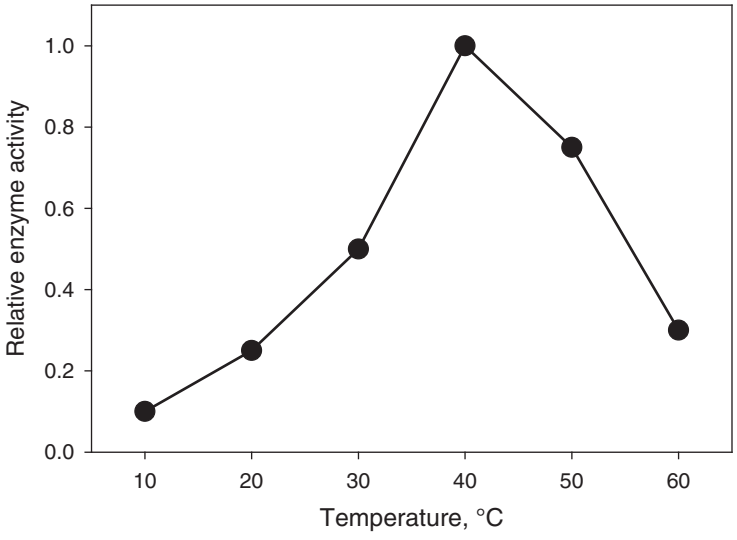


Figure 1.15 A typical temperature activity curve for enzymes shows that most exhibit peak activity near physiological temperatures. Source: Adapted from Copeland [5].

If one restricts attention to the temperature range over which protein denaturation is not significant, the rate of reaction can be related to the activation energy for attaining the reaction transition state E_a (see Figure 1.5) by the Arrhenius equation:

$$k_1' = \frac{k_B \cdot T}{h} \cdot e^{-\frac{E_a}{R \cdot T}} \tag{1.94}$$

where k_B is the Boltzmann constant (see Equation 1.58) and h is the Planck's constant ($6.626'070'15 \cdot 10^{-34}$ $m^2 \cdot kg/s$ [or J/Hz]). R and T refer to the ideal gas constant and the absolute temperature, respectively (see Equation 1.30). Thus, if one plots $\log(k_1')$ of an enzyme reaction as a function of $1/(2.3 \cdot R \cdot T)$, Equation 1.94 predicts that one will obtain a straight-line relationship with a slope equal to $-E_a$.

pH conditions: The pH of an enzyme solution can modulate its catalytic activity through multiple mechanisms. As protein molecules, enzymes possess a

(Continued)

(Continued)

native tertiary structure that is intrinsically sensitive to pH and are consequently prone to denaturation under highly acidic or highly alkaline conditions. Although most enzymes preserve their conformational stability across a relatively broad pH interval of approximately four to five units, their reaction velocities nonetheless fluctuate within this range. Figure 1.16 presents a representative profile of enzymatic activity as a function of pH under conditions in which denaturation is minimal. A detailed understanding of this pH activity relationship is essential for establishing optimal assay parameters, as the specific dependence is characteristic of each enzyme.

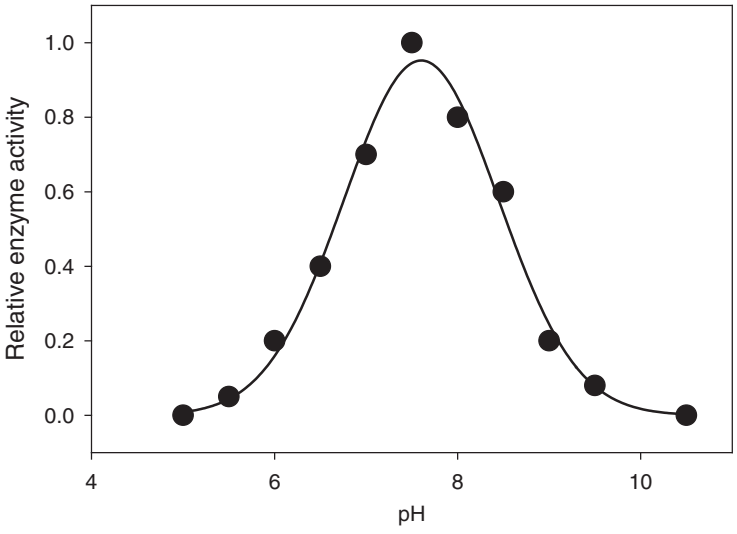


Figure 1.16 The influence of pH on the velocity of a typical enzymatic. Source: Adapted from Copeland [5]. For most enzymes, catalytic efficiency reaches its maximum within a narrow pH interval. Consequently, in general enzyme assays, it is important to maintain the solution pH at the optimum for catalysis. To achieve this, the reaction mixture must be buffered with a component whose pK_a closely matches the desired pH (see Section 1.4).

Other potential parameters known to have an influence on reaction velocity (such as ion strength and solution viscosity) are discussed in Copeland [5].

Thus, at the start of reaction, there is no product (i.e., $C(P_0) = 0$). At infinite time, the maximum amount of product that can be produced is defined by the starting concentration of substrate. Hence, at infinite time $C(P_\infty) = C(S_0)$. At any time between 0 and infinity, we must have conservation of mass, so that:

$$C(S)_t + C(P)_t = C(S)_0 \tag{1.95}$$

Using Equation 1.91, one can recast Equation 1.95 as follows:

$$C(P)_t = C(S)_0 - C(S)_0 \cdot e^{-k_1' \cdot t} = C(S)_0 \cdot \left(1 - e^{-k_1' \cdot t}\right) \tag{1.96}$$

Hence, the substrate depletion curve is the mirror image of the product appearance curve, as illustrated in Figure 1.14. The time to reduce $C(S)$ to half of its original value (i.e., the half-life of the reaction) can be determined in alignment with Equation 1.14:

$$t_{1/2} = \frac{-\ln 0.5}{k_1'} = \frac{0.693}{k_1'} \tag{1.97}$$

Initial Rate of Reaction!

Looking more carefully at the progression curve profile for an enzyme-catalyzed reaction (Figure 1.17), one realizes that in the very early portion of this plot that the increase in product formation (and the substrate depletion as well) tracks approximately linear with time. For this limited time period, the initial velocity

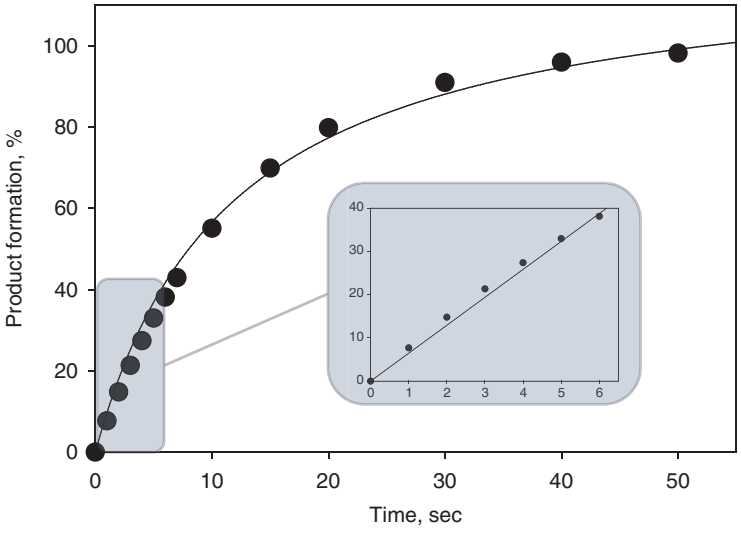


Figure 1.17 Progress (product formation) curve for an enzyme reaction. The slope in the initial rate period is the initial rate of reaction (v_0), as shown in the inset. Being relatively free from complications such as back-reaction and enzyme degradation, the initial rate experiment is the simplest to perform and analyze. It is therefore not surprising that most enzyme (and transporter) studies concentrate on this initial, approximately linear part of enzyme reactions. The length of the initial rate period depends on the assay conditions and can range from milliseconds to hours (typically up to the time when about 10% of initial substrate concentration has been converted to product). The experimental conditions where the enzymes are expected to "produce" product *M* (or "consume" the substrate *S*) at an initial rate can be summarized as follows: (i) metabolite (product) formation experiments (which should not result in a loss of >20% substrate) are preferred over substrate disappearance assessments, (ii) substrate concentration should be much less in comparison to enzyme involved in the reaction, and (iii) <1% organic solvent in incubation matrix [13].

(Continued)

(Continued)

(v_0) can be approximated as the slope of the linear plot of $C(S)$ or $C(P)$ as a function of time:

$$\vartheta_0 = -\frac{\Delta C(S)}{dt} = \frac{\Delta C(P)}{dt} \tag{1.98}$$

"Initial" here is taken to mean that the reaction rate is measured after a relatively short time period, during which it is assumed that the enzyme-substrate complex has formed, but that the substrate concentration held approximately constant, and so the equilibrium or quasi-steady-state approximations as discussed in Section 1.1.3 remains valid.

1.3.2.2 Mathematical Frameworks of Enzyme Reactions

Enzyme kinetic models generally argue that enzyme-catalyzed reactions could be best described by a reaction scheme where a substrate drug S binds reversible to an enzyme E to form a complex ES which, following a catalytic chemical reaction, breaks down to give a new product M and to release the enzyme E (Figure 1.18).

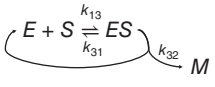


Figure 1.18 Reaction scheme for enzyme catalysis. k_{13} and k_{31} are the (association [on] and dissociation [off]) rate constants, whereas k_{32} is the rate constant for the release (catalysis) of M.

1.3.2.2.1 Rapid Equilibrium Model of Enzyme Kinetics (Henri–Michaelis–Menten Approach) This concept assumes that a rapid equilibrium is established between the reactants ($E + S$) and the ES complex, followed by slower conversion of the ES complex back to the free enzyme and product so that $k_{32} \ll k_{13}$ in the scheme presented in Figure 1.18. Hence, the equilibrium constant for the complex formation is given with (compare Equation 1.33):

$$K_d = \frac{k_{31}}{k_{13}} = \frac{C(E) \cdot C(S)}{C(ES)} \tag{1.99}$$

Since substrate depletion is typically insignificant under equilibrium conditions, similar to the relationships discussed in Section 1.3.1.1.1, one can make the approximation that $C(S) \approx C(S)_{tot}$. Expressing the free enzyme concentration by the difference between total enzyme concentration $C(E)_{tot}$ and the concentration of the binary complex $C(ES)$ one gets:

$$K_d = \frac{k_{31}}{k_{13}} = \frac{(C(E)_{tot} - C(ES)) \cdot C(S)}{C(ES)} \tag{1.100}$$

Or:

$$C(ES) = \frac{C(E)_{tot} \cdot C(S)}{K_d + C(S)} \tag{1.101}$$

The rate of product formation can be given by the first-order equation:

$$\overline{\vartheta} = \frac{dC(M)}{dt} = k_{32} \cdot C(ES) \tag{1.102}$$

Hence, combining Equations 1.101 and 1.102, one obtains a relationship describing the reaction velocity as a hyperbolic function of $C(S)$, with a maximum value of $k_{32} \cdot C(E)_{tot}$ at infinite $C(S)$:

$$\overline{\vartheta} = \frac{k_{32} \cdot C(E)_{tot} \cdot C(S)}{K_d + C(S)} \tag{1.103}$$

This relationship is conceptionally equivalent to the previously discussed Langmuir isotherm (see Equation 1.83). With $k_{32} \cdot C(E)_{tot}$ being the maximal rate of the overall reaction at saturation concentration ($\overline{V}_{max}$), one therefore gets:

$$\overline{\vartheta} = \frac{\overline{V}_{max} \cdot C(S)}{K_d + C(S)} = \frac{\overline{V}_{max}}{1 + \frac{K_d}{C(S)}} \tag{1.104}$$

Or, by accounting for the (organ, tissue, compartment, or incubation) volume where the catalytic activity occurs (V_x, compare Table 1.1):

$$\vartheta = \overline{\vartheta} \cdot V_x = \frac{\overline{V}_{max} V_x \cdot C(S)}{C(S) + K_d} = \frac{V_{max} \cdot C(S)}{C(S) + K_d} = \frac{V_{max}}{1 + \frac{K_d}{C(S)}} \tag{1.105}$$

1.3.2.2.2 Steady-State Model of Enzyme Kinetics (Michaelis–Menten Theory) According to Michaelis–Menten, the overall dynamic in a reaction system according to Figure 1.14 can also be described by the following reaction equations:

$$\frac{dC(S)}{dt} = -k_{13} \cdot C(E)_t \cdot C(S)_t + k_{31} \cdot C(ES)_t \tag{1.106}$$

$$\frac{dC(E)}{dt} = -k_{13} \cdot C(E)_t \cdot C(S)_t + k_{31} \cdot C(ES)_t + k_{32} \cdot C(ES)_t \tag{1.107}$$

$$\frac{dC(ES)}{dt} = k_{13} \cdot C(E)_t \cdot C(S)_t - k_{31} \cdot C(ES)_t - k_{32} \cdot C(ES)_t \tag{1.108}$$

$$\frac{dC(M)}{dt} = k_{32} \cdot C(ES)_t = \overline{\vartheta} \tag{1.109}$$

where $C(S)$, $C(E)$, and $C(ES)$ are the concentrations of the free (not enzyme-bound) substrate, free (not substrate-bound) enzyme and the enzyme–substrate complex, respectively. To solve these equations, one has to differentiate between three different and distinct reactions phases as follows (compare Figure 1.14): (i) a short run-in (pre-steady-state) phase with decreasing enzyme (but unaffected substrate) concentration to form the enzyme-substrate complex, (ii) a second (quasi steady-state) phase where the enzyme-substrate complex remains largely constant (i.e., $\overline{\vartheta}$ achieves its maximum), and (iii) a terminal (post-steady-state) phase characterized by the decay of the enzyme-substrate complex due to substrate depletion (i.e., where $\overline{\vartheta}$ decreases again). The duration of the different phases mainly depends on the relative contributions of three reaction rate constants. When $k_{13} \approx k_{31} \approx k_{32}$, the duration of the quasi steady-state phase is relatively short. However, when $k_{13} \approx k_{31} > k_{32}$, the quasi steady-state phase increases significantly

meaning that the enzyme–substrate complex remains constant for a considerable period of time paralleled by a linear decrease and increase of substrate and product, respectively (i.e., a situation with zero-order according to Equations 1.22–1.26). For the enzyme–substrate complex under steady-state conditions follows that $dC(ES)/dt = 0$ and consequently, assuming absence of substrate depletion (i.e., $C(S) \approx C(S)_{tot}$ [compare Equation 1.79]), Equation 1.108 can be simplified as:

$$k_{13} \cdot C(ES) \cdot C(S)_t \approx k_{13} \cdot C(ES) \cdot C(S) = (k_{31} + k_{32}) \cdot C(ES) \tag{1.110}$$

Or, in simplified form:

$$C(ES) = \frac{k_{13}}{k_{31} + k_{32}} \cdot C(E) \cdot C(S) = \frac{C(E) \cdot C(S)}{\frac{k_{31}+k_{32}}{k_{13}}} = \frac{C(E) \cdot C(S)}{K_m} \tag{1.111}$$

The (dissociation) constant K_m (with dimension of mass/volume [e.g., mmol/mL]) used for protein-catalyzed reactions is known as the Michaelis–Menten constant (note – in the context of protein-catalyzed reactions the corresponding association constant is rarely applied). Hence:

$$K_m \cdot C(ES) = C(E) \cdot C(S) \tag{1.112}$$

Following replacement of $C(E)$ with $C(E)_0 - C(ES)$, Equation 1.111 can be recast as follows:

$$K_m \cdot C(ES) = C(E)_0 \cdot C(S) - C(ES) \cdot C(S) \tag{1.113}$$

where $C(E)_0$ is the (total) enzyme concentration at $t = 0$ which, assuming no change in enzyme expression over time, is equivalent to the total enzyme concentration $C(E)_{tot}$. Solving for $C(ES)$ therefore provides (compare Equations 1.81 and 1.101):

$$\begin{aligned} C(ES) &= \frac{C(E)_{tot} \cdot C(S)}{C(S) + K_m} = \frac{C(E)_{tot} \cdot C(S)}{C(S) + \frac{1}{K_m}} = \frac{C(E)_{tot} \cdot K_m \cdot C(S)}{K_m \cdot C(S) + 1} \\ &= \frac{C(E)_{tot} \cdot C(S)}{C(S) + \frac{k_{31}+k_{32}}{k_{13}}} = \frac{k_{13} \cdot C(E)_{tot} \cdot C(S)}{k_{13} \cdot C(S) + k_{31} + k_{32}} \end{aligned} \tag{1.114}$$

Combining Equations 1.109 and 1.114 gives:

$$\overline{\vartheta} = \frac{dC(M)}{dt} = k_{32} \cdot C(ES) = \frac{k_{32} \cdot C(E)_{tot} \cdot C(S)}{C(S) + K_m} \tag{1.115}$$

The maximum catalytic activity of the enzyme is reached when all enzyme is involved in the ES complex (i.e., when $C(ES) = C(E)_{tot}$). Consequently, $k_{32} \cdot C(E)_{tot}$ is equal to the maximal rate of the overall reaction at saturation concentration $\left(\overline{V}_{max}\right)$ to give:

$$\overline{\vartheta} = \frac{dC(M)}{dt} = k_{32} \cdot C(ES)_{tot} = \frac{\overline{V}_{max} \cdot C(S)}{C(S) + K_m} = \frac{\overline{V}_{max}}{1 + \frac{K_m}{C(S)}} \tag{1.116}$$

Or, in alignment with Equation 1.105:

$$\vartheta = \overline{\vartheta} \cdot V_x = \frac{\overline{V}_{max} V_x \cdot C(S)}{C(S) + K_m} = \frac{V_{max} \cdot C(S)}{C(S) + K_m} = \frac{V_{max}}{1 + \frac{K_m}{C(S)}} \tag{1.117}$$

Relationships Equations 1.116 and 1.117 are generally referred to as Michaelis–Menten equations.

Note!

For enzymes with multiple identical binding sites in accordance with Equations 1.89, 1.116, requires rewriting as follows:

$$\overline{\vartheta} = \frac{dC(M)}{dt} = n \cdot \frac{\overline{V}_{max} \cdot C(S)}{C(S) + K_m} \tag{1.118}$$

Accordingly, for enzymes with multiple non-identical binding sites according to Equation 1.90, one gets:

$$\overline{\vartheta} = \frac{dC(M)}{dt} = \sum_{i=1}^{x} n_i \cdot \frac{\overline{V}_{max,mi} \cdot C(S)}{C(S) + K_{m,mi}} \tag{1.119}$$

It should be noted that the value of $\overline{V}_{max}$ $\left(or\ V_{max}\right)$, in contrast to K_m $(=(k_{31} + k_{32})/k_{13}$ [see Equation 1.114]), is dependent on the (total) concentration of the enzyme. In comparing Equation 1.116 for steady-state kinetics with Equation 1.104 for rapid equilibrium treatment, one sees that the relationships are identical for the substitution of K_m for K_d in the steady-state treatment. It is therefore easy to confuse these terms. However, the two constants are not always equal, even in consideration of the simplest reaction schemes as here. Only under the specific conditions that $k_{32} \ll k_{13}$ are K_m and K_d $(=k_{31}/k_{13}$ [see Equation 1.99]) equivalent. Hence, depending on the details of the reaction mechanism and the values of the individual rate constants, situations can arise in which the value of K_m is less than, greater than, or equal to K_d. Therefore, K_m should generally be considered as a kinetic, not thermodynamic, constant. This rationalizes the fact that the Michaelis–Menten model is generally accepted as the most suitable approach for the description of enzyme kinetics.

Turnover Number and Specificity Constant!

In the simplest Michaelis–Menten case according to Equation 1.115, a single chemical step, defined by the first-order rate constant k_{32}, results in product formation, as depicted in Figure 1.18. More likely, however, there will be a series of rapid chemical events following ES complex formation (compare Section 1.1.3). For simplicity, the overall rate for these collective chemical steps can be described by a single first-order rate constant called k_{cat}. Hence, the maximal rate of product formation is given by $k_{cat} \cdot C(E)_{tot}$ and the expression for velocity according to Equation 1.115 must be rewritten as:

$$\overline{\vartheta} = \frac{\overline{V}_{max} \cdot C(S)}{C(S) + K_m} = \frac{k_{cat} \cdot C(E)_{tot} \cdot C(S)}{C(S) + K_m} \tag{1.120}$$

(Continued)

(Continued)

Consequently, the turnover number of an enzyme, or the k_{cat}, is the maximal number of molecules of substrate converted to product per active site per unit time when the enzyme is saturated with substrate. In the laboratory, one can easily determine the turnover as $k_{cat,}$ by measuring the reaction velocity under conditions of $C(S) \gg K_m$ so that $\bar{\nu}$ approaches $\overline{V}_{max}$. The rate of enzyme turnover under most physiological conditions in vivo, however, is very different from the laboratory situation. in vivo, the concentration of substrate is more typically 0.1–1 times the K_m value. When $C(S) \ll K_m$, the expression for velocity changes to:

$$\overline{\vartheta} = \frac{k_{cat}}{K_m} \cdot C(E)_{tot} \cdot C(S) \tag{1.121}$$

where the k_{cat}/K_m value (with units of a second-order rate constant), or specificity constant, is probably the best measure of the catalytic efficiency of an enzyme allowing to compare efficiencies of different enzymes to one another (i.e., that substrate with the highest value is the best substrate for the enzyme). Recalling Equation 1.114 we note that:

$$\frac{k_{cat}}{K_m} = \frac{k_{cat} \cdot k_{13}}{k_{31} + k_{cat}} \tag{1.122}$$

Thus, under laboratory conditions, where $C(S) \gg K_m$, formation of the ES complex is rapid and often not the rate-limiting step. in vivo, however, where $C(S) \ll K_m$, the overall reaction may be limited by the diffusional rate of encounter of free enzyme with substrate, which is defined by k_{13}. Enzymatic reactions are in principle reversible, although for many enzymes the reverse reaction is thermodynamically unfavorable (compare Section 1.1.2). Thus, the k_{cat}/K_m ratio can also be used to compare efficiency with which an enzyme catalyzes a particular reaction in the forward and reverse directions. At equilibrium (eq), the forward (f) and reverse (r) reactions occur with equal frequency so that with reference to Equation 1.121 follows:

$$\left(\frac{k_{cat}}{K_m}\right)_f \cdot C(E)_{tot} \cdot C(S)_{eq} = \left(\frac{k_{cat}}{K_m}\right)_r \cdot C(E)_{tot} \cdot C(M)_{eq} \tag{1.123}$$

Hence, for the equilibrium constant K_{eq} between the substrate and the product concentrations, Equation 1.124 follows:

$$K_{eq} = \frac{C(M)_{eq}}{C(S)_{eq}} = \frac{\left(\frac{k_{cat}}{K_m}\right)_f}{\left(\frac{k_{cat}}{K_m}\right)_r} \tag{1.124}$$

Equation 1.124, known as Haldane relationship, provides a useful measure of the directionality of an enzyme reaction under a specific set

of solution conditions. Integration of Equation 1.121 provides (compare Equation 1.92):

$$C(S)_t = C(S)_0 \cdot e^{-\frac{k_{cat}}{K_m} \cdot C(E)_{tot} \cdot t} \tag{1.125}$$

Comparing Equation 1.125 with Equation 1.92 we see that for $C(S) \ll K_m$:

$$k_1' = \frac{k_{cat}}{K_m} \cdot C(E)_{tot} \tag{1.126}$$

1.3.2.2.3 The Intrinsic Clearance Concept Equations 1.116 and 1.117 exhibit a hyperbolic rate vs. substrate concentration relationship, as illustrated in Figure 1.19 (panel A). The resultant curve can basically be divided into two main parts (or zones) – a first part where the rate of the catalytic reaction almost linearly increases with the substrate concentration (i.e., a concentration-dependent reaction zone typically referred to as first-order, linear, or non-saturated part [compare Equation 1.4]) and a second part where the rate of reaction approaches a maximum velocity asymptotically so that it becomes approximatively independent of the substrate concentration (i.e., a concentration-independent reaction zone typically referred to as zero-order, constant, or saturated part [see Equation 1.22]). The proportionality factor between the velocity of a catalytic reaction (ϑ) and the substrate concentration ($C(S)$), in alignment with Equation 1.75, is typically referred to as (metabolic) intrinsic clearance ($CL_{int,met}$ or just CL_{int}). Therefore, for every specific organ/tissue (x), the Michaelis–Menten Equations 1.116 and 1.117 can be rewritten as follows (Figure 1.19 (panel B)):

$$\begin{aligned} CL_{int,x} &= \frac{\vartheta_x}{C(S)_x} = \frac{\overline{\vartheta}_x \cdot V_x}{C(S)_x} = \frac{\overline{V}_{max,x} \cdot V_x}{C(S)_x + K_m} = \frac{V_{max,x}}{C(S)_x + K_m} \\ &= \frac{V_{max,x}}{C(S)_x + \frac{1}{K_{m,a}}} = \frac{K_{m,a} \cdot V_{max,x}}{K_{m,a} \cdot C(S)_x + 1} \end{aligned} \tag{1.127}$$

For $C(S)_x \gg K_m$, the relationship approaches the zero value with:

$$CL_{int,x} = \frac{V_{max,x}}{C(S)_x} = \frac{\overline{V}_{max,x} \cdot V_x}{C(S)_x} = \frac{const}{C(S)_x} \tag{1.128}$$

For $C(S)_x \ll K_m$, representing a low reaction rate situation (reaction is assumed not to show saturability as shown in Figure 1.19), the expression simplifies to:

$$CL_{int,x} = \frac{\overline{V}_{max,x} \cdot V_x}{\mathrm{K}_m} = \frac{V_{max,x}}{K_m} = K_{m,a} \cdot V_{max,x} = const \tag{1.129}$$

The clearance term according to Equations 1.127–1.129 gives an indication of how efficiently a drug is metabolized by an enzyme (or the totality of enzymes) of a particular tissue, e.g., the liver. The highest intrinsic clearance value according to Equation 1.129 is typically used as a theoretical measure for a drug's maximal elimination rate by an organ.

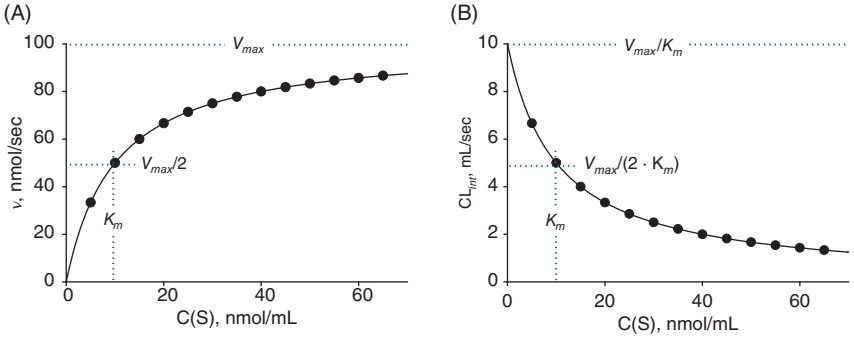


Figure 1.19 Panel A: When metabolism follows Michaelis–Menten kinetics, the rate of metabolism or elimination (v) increases toward a maximum value V_{max} (hyperbolic saturation curve) as the drug or substrate concentration $C(S)$ is increased (compare Equations 1.116 and 1.117). The concentration at which the rate is one-half, the maximum is the K_m value. Panel B: The corresponding (metabolic or metabolite) intrinsic clearance CL_{int} ($= v/C(S)$), drops with increasing intracellular concentration (compare Equation 1.127). The concentration at which intrinsic metabolic clearance is one-half, the maximum is also the K_m value.

Determination of Enzyme Kinetic Constants!

Most methods for the determination of the kinetic constants (V_{max} and K_m and, hence, CL_{int}) involve running a series of enzyme reaction experiments under initial reaction rate conditions at varying substrate concentrations $C(S)$ to determine the rate of metabolism vs. concentration relationships as depicted in Figure 1.19 (panel A).

Reaction curve fitting (*nonlinear regression*)*:* In this approach, the kinetic constants are determined graphically using nonlinear regression of the Michaelis–Menten relationship (see Equations 1.116 and 1.117).

Graphical methods involving linearization: Before computing facilities to perform nonlinear regression became available, graphical methods involving linearization of the Michaelis–Menten equation were used.

The most popular, so-called Lineweaver–Burk (or double reciprocal) approach is to employ the double-reciprocal plot of $1/v_0$ vs. $1/C(S)$. From Equation 1.117, we write:

$$\frac{1}{\vartheta} = \frac{1}{\frac{V_{max}}{1+\frac{K_m}{C(S)}}} = \frac{1+\frac{K_m}{C(S)}}{V_{max}} = \frac{1}{V_{max}} + \frac{K_m}{V_{max} \cdot C(S)} \tag{1.130}$$

Based on this relationship, both V_{max} and K_m can be obtained from the slope and the intercepts of the straight line, as shown in Figure 1.20 (panel A). Although useful and widely employed in enzyme/transporter kinetic studies,

the Lineweaver-Burk method has the disadvantage of compressing the data points at high substrate concentrations into a small region and emphasizing the points at lower substrate concentrations, which are often the least accurate. Another way of plotting the kinetic data is obtained by multiplying both sides of Equation 1.130 by the product $\vartheta \cdot V_{max}$:

$$\frac{\vartheta \cdot V_{max}}{\vartheta} = \frac{\vartheta \cdot V_{max}}{V_{max}} + \frac{(\vartheta \cdot V_{max}) \cdot K_m}{V_{max} \cdot C(S)} = \vartheta + \frac{\vartheta \cdot K_m}{C(S)} \tag{1.131}$$

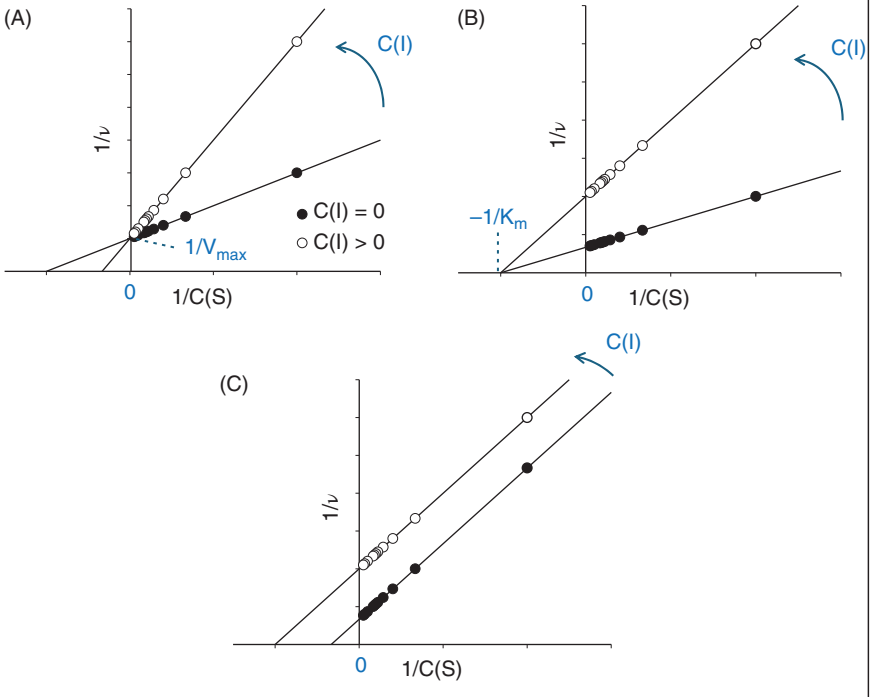


Figure 1.20 Graphical determination of enzyme reaction constants for single-substrate reactions obeying Michaelis–Menten kinetics using linearization approaches according to Lineweaver–Burk (panel A), Eadie–Hofstee (panel B), and Hanes–Woolf (panel C). For illustration purposes, the same data points as in Figure 1.19 were used.

Rearrangement gives:

$$\vartheta = V_{max} - \frac{\vartheta \cdot K_m}{C(S)} \tag{1.132}$$

This equation shows that a plot of v_0 vs. $v_0/C(S)$, the so-called Eadie–Hofstee plot, gives a straight line with slope equal to $-K_m$ and intercept V_{max} on the ϑ axis and V_{max}/K_m on the ϑ /$C(S)$ axis (Figure 1.20 (panel B)). A third

(Continued)

(Continued)

transformation that is commonly used is obtained by multiplying both sides of Equation 1.130 by $C(S)$ to obtain:

$$\frac{C(S)}{\vartheta} = \frac{C(S)}{V_{max}} + \frac{C(S) \cdot K_m}{V_{max} C(S)} = \frac{C(S)}{V_{max}} + \frac{K_m}{V_{max}} \tag{1.133}$$

From this a plot of $C(S)/\vartheta$ vs. $C(S)$ yields a straight line with slope equal to $1/V_{max}$ and intercept equal to K_m/V_{max}. Figure 1.20 (panel C) illustrates such a plot, which is known as Hanes–Woolf diagram. In literature there are several other ways of plotting kinetic data. However, while useful for visualization, all methods distort the error structure of the data and are inferior to nonlinear regression. Nonetheless, their use is still widely spread. Of all approaches shown here, the Hanes–Woolf plot is the most accurate.

Drug disappearance, half-life, or stability method: This simple approach refers to only one substrate concentration and follows the initial decrease in substrate concentration over time (see Figure 1.14). Referring to Equation 1.116, for $C(S) \ll K_m$, the following applies:

$$\vartheta = \frac{dC(S)}{dt} = \frac{\overline{V}_{max} \cdot C(S)}{K_m} = \frac{ln2}{t1/2} \cdot C(S) = \frac{0.693}{t1/2} \cdot C(S) \tag{1.134}$$

where assuming first-order reaction kinetics, $t_{1/2}$ ($= \ln 2 \cdot K_m/V_{max}$ [compare Equation 1.14]) is the half-life of drug disappearance in the incubation. $t_{1/2}$ can be determined experimentally from a semi-logarithmic concentration vs. time plot as follows (compare Figure 2.2):

$$t_{1/2} = \frac{0.693 \cdot (t_2 - t_1)}{\ln\left(\frac{C_1}{C_2}\right)} \tag{1.135}$$

C_1 and C_2 are any substrate concentrations at time t_1 and t_2 after the start of incubation, respectively. Consequently, the intrinsic clearance CL_{int} can be assessed with (compare Equations 1.116 and 1.129):

$$CL_{int} = \frac{\vartheta}{C(S)} = \frac{V_{max}}{K_m} = \frac{\overline{V}_{max} \cdot V_{inc}}{K_m} = \frac{0.693}{t_{1/2}} \cdot V_{\mathrm{inc}} \tag{1.136}$$

where V_{inc} is the incubation volume. This intrinsic clearance assay approach is useful, especially when it is difficult to perform the kinetics experiment over a wide range of concentrations. The method is easier and faster than the full kinetics methods described earlier; however, it does not allow to determine K_m and V_{max} values.

Hence, the intrinsic clearance conceptually denotes the value of organ clearance one would obtain if there were no diffusion (e.g., due to protein binding [Section 4.1] or permeability [Section 3.2.2] or flow [Section 5.1.2]) limitations and is therefore generally regarded as a measure of enzyme activity within an organ/tissue, isolated from any limitations imposed by reaction saturation and events in the perfusing

blood. As such, the value of intrinsic clearance can be many orders of magnitude greater than for the organ blood flow. Inferred through the analysis of in vivo data, where one cannot measure events within the cell, and determined experimentally in vitro (see Sectionss 5.2 and 6.2.1.3), the concept of intrinsic clearance is critical to development of pharmacokinetic principles in general.

Effect of Activity Alterations on Intrinsic Clearance!

The (intrinsic) clearance might be subject to activity alterations due to a series of exogenous factors (such as inhibition and/or induction [see Section 8.1.1]) or genetic factors (i.e., inherited mutations in the gene and/or copy number variations [CNV] [compare Section 8.1.1.2]). Some of these factors (e.g., competitive reversible inhibition, gene mutations) predominantly result in an attenuation of the affinity parameter K_m, while other factors (e.g., induction and CNV) mainly have an impact on the capacity value V_{max}. In consequence the rate of reaction may increase or decrease depending on the balance of these effects, as illustrated in Figure 1.21.

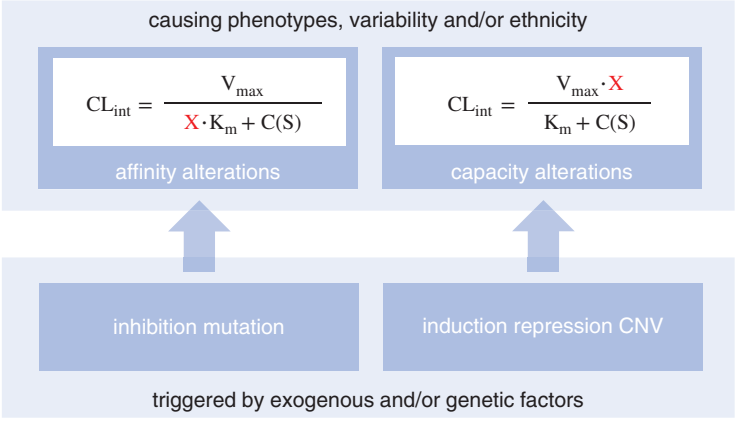


Figure 1.21 Factors impacting K_m and/or V_{max}, resulting in (intrinsic) clearance changes (compare Equation 1.127), where X denotes the correction factor for the observed change. Source: Adapted from Schiller et al. [14]. CNV = copy number variations.

When more than one catalytic protein (n) is present, assuming a parallel (not serial) arrangement, the individual intrinsic clearance relationships can be combined to provide a total (or apparent [app]) intrinsic clearance value as follows:

$$\begin{aligned} CL_{int,tot,x} &= \frac{V_{max,app,x}}{C(S)_x + K_{m,app}} = \sum_{j=1}^{n} CL_{int,j,x} \\ &= \frac{V_{max,1,x}}{C(S)_x + K_{m,1}} + \frac{V_{max,2,x}}{C(S)_x + K_{m,2}} + \cdots + \frac{V_{max,n,x}}{C(S)_x + K_{m,n}} \\ &= \sum_{j=1}^{n} \frac{V_{max,j,x}}{C(S)_x + K_{m,j}} \end{aligned} \tag{1.137}$$

Hence, the fractional contribution (*fm*) of any particular catalytic protein (e.g., enzyme $j = 2$) to overall intrinsic clearance can be estimated with:

$$fm_{2,x} = \frac{CL_{int,2,x}}{CL_{int,tot,x}} = \frac{\frac{V_{max,2,x}}{C(S)_x + K_{m,2}}}{\sum_{j=1}^{n} \frac{V_{max,j,x}}{C(S)_x + K_{m,j}}} \tag{1.138}$$

1.3.2.2.4 Atypical Enzyme Kinetics

Multiple Substrate Kinetics Until now, we have considered only the simplest of enzyme reactions, those involving a single substrate being transformed into a single product. However, often one encounters reactions involving at least two substrates, typically resulting in the formation of more than one product (note: the number of substrates and products in the reaction is specified by the terms uni, bi, ter, and quad, e.g., a reaction that uses one substrate and generates three products is called a "uni-ter" reaction). The simplest version of this reaction type, referring to a situation where the catalytic reaction with multiple substrates happens asynchronous (i.e., independently competitive), is as illustrated in Figure 1.22.

The steady-state assumptions for this reaction type are [15, 16]:

$$\frac{dC(ES_1)}{dt} = k_1 \cdot C(E) \cdot C(S_1) - (k_{-1} + k_2) \cdot C(ES_1) = 0 \tag{1.139}$$

$$\frac{dC(ES_2)}{dt} = k_3 \cdot C(E) \cdot C(S_2) - (k_{-3} + k_4) \cdot C(ES_2) = 0 \tag{1.140}$$

$$\frac{dC(M_1)}{dt} + \frac{dC(M_2)}{dt} = k_2 \cdot C(ES_1) + k_4 \cdot C(ES_2) = \overline{\vartheta} \tag{1.141}$$

$$C(E)_{tot} = C(E) + C(ES_1) + C(ES_2) \tag{1.142}$$

Replacing $C(E)$ from Equation 1.142 into Equations 1.139 and 1.140, one gets:

$$C(ES_1) = C(E)_{tot} - C(ES_2) \cdot \left(1 + \frac{k_{-3} + k_4}{k_3 \cdot C(S_2)}\right) = 0 \tag{1.143}$$

$$C(ES_2) = C(E)_{tot} - C(ES_1) \cdot \left(1 + \frac{k_{-1} + k_2}{k_1 \cdot C(S_1)}\right) = 0 \tag{1.144}$$

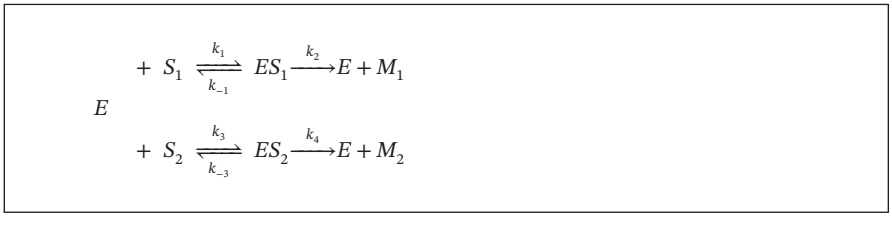


Figure 1.22 Reaction scheme for an enzyme involving two independent substrates (S_1 and S_2) resulting in two different products (M_1 and M_2) (so-called competing [i.e., alternative, sequential or either…or] bi-bi reaction mechanism, or alternative substrate competition).

Combining Equations 1.143 and 1.144 and considering that $(k_{-1} + k_2)/k_1 = Km_1$ and $(k_{-3} + k_4)/k_3 = Km_2$ provides (compare Equation 1.111):

$$C(ES_1) = \frac{Km_2 \cdot C(E)_{tot} \cdot C(S_1)}{Km_2 \cdot C(S_1) + Km_1 \cdot C(S_2) + K_{m,1} \cdot K_{m,2}} \tag{1.145}$$

$$C(ES_2) = \frac{Km_1 \cdot C(E)_{tot} \cdot C(S_2)}{Km_2 \cdot C(S_1) + Km_1 \cdot C(S_2) + K_{m,1} \cdot K_{m,2}} \tag{1.146}$$

Inserting Equations 1.145 and 1.146 into Equation 1.141 ultimately gives a new velocity relationship as follows:

$$\begin{aligned} \vartheta = \overline{\vartheta} \cdot V_x &= \frac{V_{max,1} \cdot C(S_1) \cdot K_{m,2} + V_{max,2} \cdot C(S_2) \cdot K_{m,1}}{C(S_1) \cdot K_{m,2} + C(S_2) \cdot K_{m,1} + K_{m,1} \cdot K_{m,2}} \\ &= \frac{\frac{V_{max,1} \cdot C(S_1)}{K_{m,1}} + \frac{V_{max,2} \cdot C(S_2)}{K_{m,2}}}{\frac{C(S_1)}{K_{m,1}} + \frac{C(S_2)}{K_{m,2}} + 1} \end{aligned} \tag{1.147}$$

From Equation 1.147 follows that, if two compounds are alternative substrates for a single enzyme, then the total rate of reaction for a mixture of the two compounds may be greater than the rate for either compound alone or may lie between the rates for the compounds alone. It is the concentration of the compound with the higher maximum velocity that determines which applies, and there is one concentration of the compound of higher maximum velocity at which the total rate of reaction is independent of the presence or absence of the substrate of lower maximum velocity. More complex multiple substrate kinetics refer to situations where catalytic reaction of several substrates happens simultaneously (Figure 1.23). The complexity of these models is certainly out of scope within the context of this book, and the interested reader is asked to read the relevant literature. However, although the presence of additional substrate(s) is ultimately leading to an alteration in overall reaction velocity (i.e., a change in apparent V_{max} and/or apparent K_m), it needs to be noted that all these mechanisms still can sufficiently well be characterized with the typical hyperbolic Michaelis–Menten relationship.

Non-Michaelis–Menten Kinetics It has become widely recognized that some individual enzymes do not conform to typical enzymological processes meaning that they often do not exhibit standard hyperbolic Michaelis–Menten kinetics. Reasons for this deviation from standard hyperbolic dependence are diverse and often just originate in experimental artifacts that have appearance of deviations from the expected behavior. A (more) rational cause of nonhyperbolic kinetics is the presence of more than one enzyme acting on the same substrate. Suppose the existence of two enzymes, both able to convert the substrate to the same product but displaying different kinetic constants (i.e., for one of the enzymes, $V_{max} = V_{max,1}$ and $K_m = K_{m,1}$, and for the second enzyme, $V_{max} = V_{max,2}$ and $K_m = K_{m,2}$). The velocity of overall mixture is then given as:

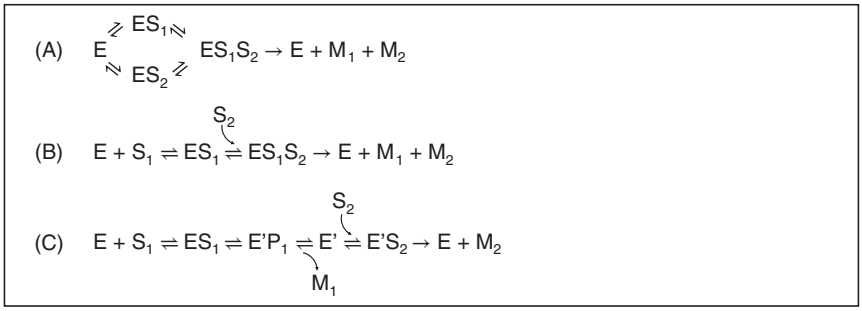


Figure 1.23 Various reaction schemes for simultaneous multi-substrate reactions. In the so-called random bi-bi reaction, the reaction of the two substrates, independent of which substrate binds first, goes through a ternary complex (ES_1S_2) (panel A). In the compulsory ordered bi-bi reaction, on the other hand, one substrate (say S_1) must bind to the enzyme before the other substrate can bind. As with the random ordered reaction, the mechanism proceeds through the formation of the ternary intermediate ES_1S_2 (panel B). The so-called double displacement (or ping-pong) bi-bi reaction mechanism involves two sequential substrate binding steps (i.e., one after the other), in which a group is transferred from one substrate to the other (panel C). In the first reaction step, the first substrate enters the active site of the free enzyme and the first product (M_1) leaves, producing a substituted enzyme ($E\prime$), in which the enzyme is bound to the group to be transferred. In the second reaction step, the second substrate enters the active site and the group on the substituted enzyme is then passed to it, producing the second product (M_2), which then leaves the active site, regenerating the free enzyme.

$$\begin{aligned}\vartheta = \overline{\vartheta} \cdot V_x &= \frac{V_{max,1} \cdot C(S)}{K_{m,1} + C(S)} + \frac{V_{max,2} \cdot C(S)}{K_{m,2} + C(S)} \\ &= \frac{(V_{max,1} \cdot K_{m,2} + V_{max,2} \cdot K_{m,1}) \cdot C(S) + (V_{max,2} + V_{max,2}) \cdot C(S)^2}{K_{m,1} \cdot K_{m,2} + (K_{m,1} + K_{m,2}) \cdot C(S) + C(S)^2}\end{aligned} \tag{1.148}$$

Equation 1.148 is a polynomial expression which yields biphasic kinetics, as illustrated in Figure 1.24.

Another type of atypical kinetic phenomenon species is known as substrate inhibition (SI). SI is thought to occur due to a second substrate molecule binding to the ES complex to form an inactive (inhibitory) ternary complex SES, as illustrated in Figure 1.25.

In alignment with Equation 8.29 (i.e., by replacing $C(I)$ with $C(S)$), the so-called Haldane Equation has been derived to describe the kinetics of enzyme-catalyzed reactions that exhibit substrate inhibition as follows [17]:

$$\begin{aligned}\vartheta = \overline{\vartheta} \cdot V_x &= \frac{V_{max} \cdot C(S)}{K_m + C(S) \cdot \left(1 + \frac{C(S)}{K_{SI}}\right)} = \frac{V_{max} \cdot C(S)}{K_m + C(S) + \frac{C(S)^2}{K_{SI}}} \\ &= \frac{V_{max}}{1 + \frac{K_m}{C(S)} + \frac{C(S)}{K_{SI}}} = \frac{\frac{V_{max} \cdot C(S)}{K_m}}{1 + \frac{C(S)}{K_m} + \frac{C(S)^2}{K_m \cdot K_{SI}}}\end{aligned} \tag{1.149}$$

Figure 1.26 illustrates the type of (bilinear parabolic) behavior one might see for an enzyme that exhibits substrate inhibition.

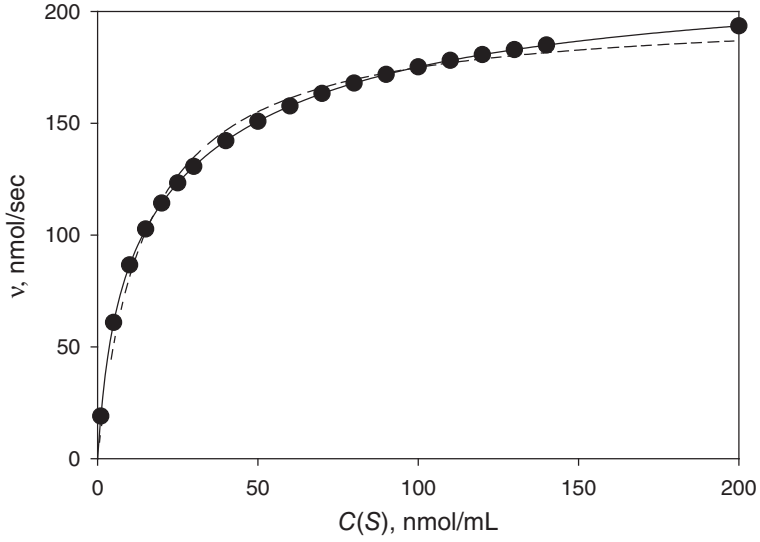


Figure 1.24 Relationship between catalytic activity and substrate concentration for two enzymes acting on the same substrate (example with $V_{max,1} = 100$ nmol/sec, $K_m = 5$ nmol/mL, $V_{max,2} = 120$ nmol/sec and $K_{m2} = 50$ nmol/mL). The solid line represents the fit of the data to the biphasic Equation 1.148, while the dashed line represents the fit of the same data to the hyperbolic Michaelis–Menten model for a single enzyme according to Equation 1.117.



Figure 1.25 Substrate inhibition model where an enzyme *E* can bind one (*ES*) or two (*SES*) substrate molecules (*S*). The equilibria for the first and second substrate molecules are described by the Michaelis–Menten constant K_m and the inhibition constant K_{SI}, respectively (compare Sections 1.3.2.2.2 and 8.1.1.1.1). k_{cat} = collective rate constant (compare Section 1.3.2.2.2).

Nonhyperbolic behavior can also be caused by catalytic regulation, referring to altered multi-site kinetics by binding an effector molecule (i.e., a modulator molecule [ε] that selectively binds to a protein to regulate its biological activity) at distance sites (i.e., at a site other than the enzyme's active site) whereby the regulatory binding site can be another active site (typically assumed to be on a different protein subunit, in this case the effector is usually a substrate and one refers to cooperativity) or any site not being an active site (typically assumed to be on the same protein subunit, in this case the effector is usually a non-substrate and one refers to allostery or allosteric regulation as discussed in Section 8.1.1.1). Cooperativity caused by only one substrate type present is referred to as autoactivation (or homotropic cooperativity). Homotropic cooperativity is thought to occur due to

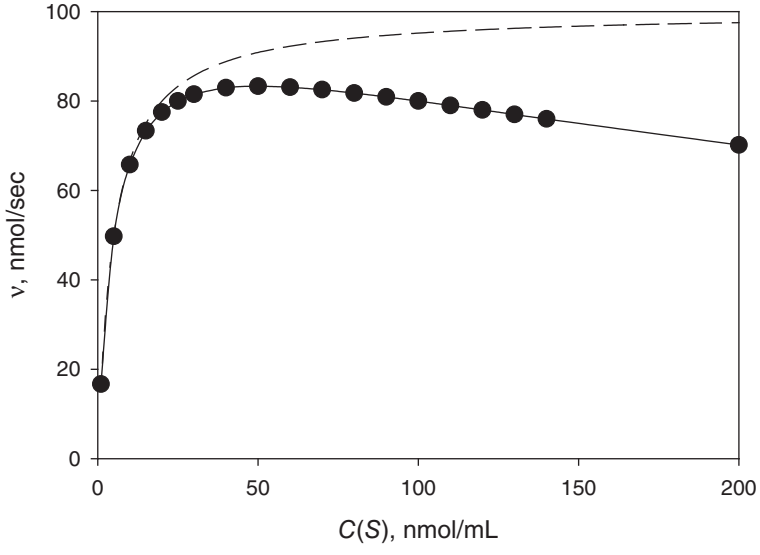


Figure 1.26 Kinetic profile of a drug metabolism process exhibiting substrate inhibition. The solid line represents substrate inhibition according to the bilinear parabolic Equation 1.149 (example with $V_{max} = 100$ nmol/sec, $K_m = 5$ nmol/mL and $K_{SI} = 500$ nmol/mL), while the dashed line shows the corresponding (i.e., same V_{max} and K_m) Michaelis–Menten relationship according to Equation 1.117. Because formation of the ES complex must precede formation of the inhibitory SES complex, substrate inhibition is usually realized only at higher substrate concentration.

the presence of multiple binding regions within the enzyme. However, it is unclear whether metabolism of the substrate occurs from either binding site or whether the presence of a second substrate molecule binding within the active site produces a change in enzyme efficiency such that metabolism of substrate molecules in the primary binding region becomes increased. Homotropic cooperativity typically results in a sigmoidal kinetic profile as depicted in Figure 1.27.

A mechanism-dependent sigmoidal model for homotropic cooperativity was presented by [18]:

$$\vartheta = \overline{\vartheta} \cdot V_x = \frac{\frac{V_{max,1} \cdot C(S)}{K_{m,1}} + \frac{V_{max,2} \cdot C(S)^2}{K_{m,1} \cdot K_{m,2}}}{1 + \frac{C(S)}{K_{m,1}} + \frac{C(S)^2}{K_{m,1} \cdot K_{m,2}}} = \frac{V_{max,1} \cdot C(S) \cdot K_{m,2} + V_{max,2} \cdot C(S)^2}{K_{m,1} \cdot K_{m,2} + \cdot C(S) \cdot K_{m,2} + C(S)^2} \tag{1.150}$$

where $K_{m,1}$ and $K_{m,2}$ are Michaelis constants for binding of the first and second substrate molecules, and $V_{max,1}$ and $V_{max,2}$ are the respective maximal velocities. On the other hand, so-called heterotropic cooperativity is thought to occur due to the presence of multiple discrete binding regions within the enzyme so that metabolism of the object substrate (S_1) is increased in the presence of a second (but different) effector substrate (S_2). The mechanism-dependent sigmoidal relationship

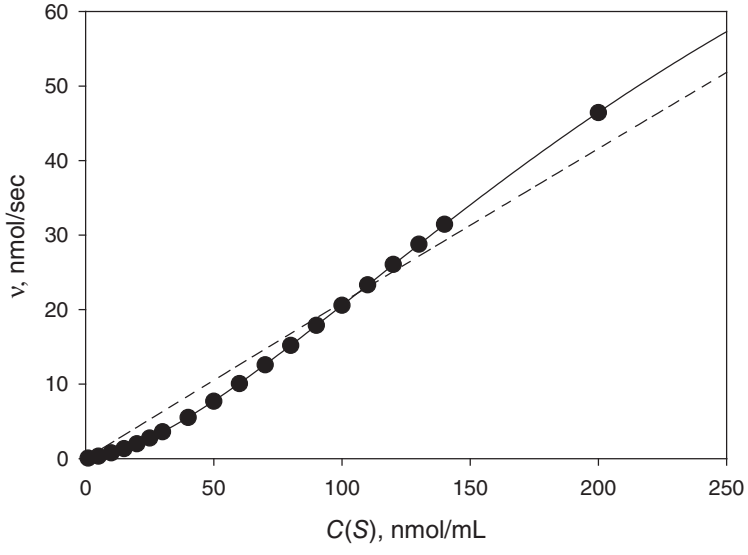


Figure 1.27 Relationship between catalytic activity and substrate concentration for a cooperative drug metabolism process exhibiting a sigmoidal profile (example with V_{max},1 = 10 nmol/sec, K_m = 200 nmol/mL, V_{max},2 = 150 nmol/sec, and K_{m2} = 250 nmol/mL). Data were fitted to both an autoactivation model (solid line, Equation 1.150) as well as the Michaelis–Menten model (dashed line, Equation 1.117).

for the metabolism of diverse substrates from two sites within the enzyme is given as [19]:

$$\vartheta = \overline{\vartheta} \cdot V_x = \frac{V_{max,S1} \cdot C(S_1)}{K_{m,S1} \cdot \frac{\left(1+\frac{C(S_2)}{K_{m,S2}}\right)}{\left(1+\frac{\beta \cdot C(S_2)}{\alpha \cdot K_{m,S2}}\right)} + C(S_1) \cdot \frac{\left(1+\frac{C(S_2)}{\alpha \cdot K_{m,S2}}\right)}{\left(1+\frac{\beta \cdot C(S_2)}{\alpha \cdot K_{m,S2}}\right)}} \tag{1.151}$$

where $K_{m,S1}$ and $K_{m,S2}$ are Michaelis constants for binding of S_1 and S_2, respectively. $V_{max,S1}$ is the maximal velocity in the presence of S_1 only, while α and β are non-physiological correction factors to reflect the changes in $K_{m,S1}$ and $V_{max,S1}$ due to cooperativity/effector binding, respectively. From Equations 1.149–1.151, it becomes evident that in order to model cooperativity phenomena, a number of data points need to be collected at a variety of substrate and effector concentrations. However, non-Michaelis–Menten (sigmoidal or bilinear) concentration vs. velocity relationships can often sufficiently be determined by modifying the Michaelis–Menten equation according to Hill (compare Equation 7.10):

$$\vartheta = \overline{\vartheta} \cdot V_x = \frac{V_{max} \cdot C(S)^n}{\alpha \cdot K_m + C(S)^n} \tag{1.152}$$

where n is the so-called Hill coefficient reflecting the (theoretical) number of binding sites (Figure 1.28).

In summary, atypical kinetics is difficult to characterize. In any case, quantitative models that account for atypical kinetics are required. Without such models,

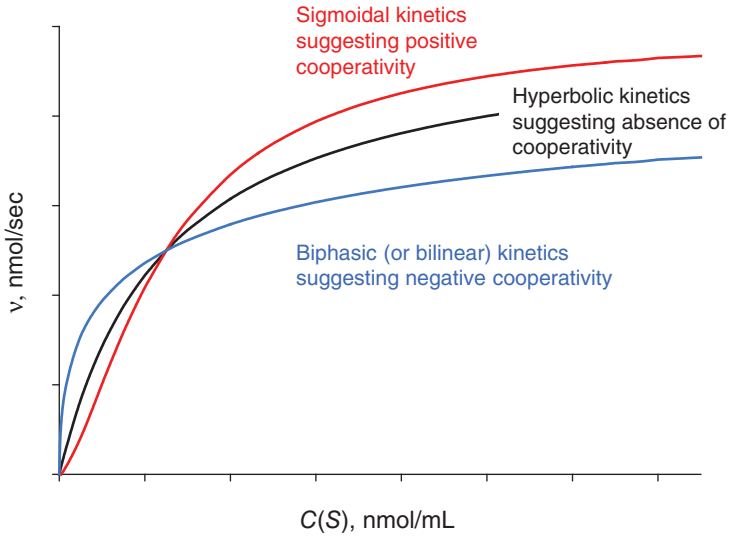


Figure 1.28 Rate of reaction vs. substrate concentration relationships according to Equation 1.152 with sigmoidal (for $n > 1$) or hyperbolic ($n \leq 1$) dependences depending on the degree and type of cooperativity. Coefficient numbers greater than one ($n > 1$) indicate positive cooperativity, i.e., the binding of a substrate molecule to one active site increases the affinity for substrate of the other active sites. Numbers less than one ($n < 1$) indicate negative cooperativity, i.e., the binding of substrate to one active site lowers the affinity of the other active sites for substrate binding, while a coefficient equal to one ($n = 1$) indicates that the affinity of the enzyme for a substrate molecule is not dependent on whether or not other substrate molecules are already bound.

in vitro kinetics will be parameterized inaccurately, intrinsic (and consequently also in vivo) drug clearance could be estimated incorrectly, and drug–drug interactions will be more difficult to predict (see Chapter 8). Nevertheless, the complexity of these models is out of scope within the context of this book, and the interested reader is asked to read the relevant literature. Thus, metabolism discussions in this textbook typically refer to Michaelis–Menten kinetics only.

Species Differences in Metabolism!

Animal models are commonly used in the preclinical development of new drugs to predict the metabolic behavior of new compounds in humans. It is, however, important to realize that humans differ from animals with regards to isoform composition, expression (compare Appendix E), and catalytic activities of drug-metabolizing enzymes. The most important drug-metabolizing enzyme family, CYP, is one of the conserved entities among species. CYP appears to be derived from a single ancestral gene from >1 billion years ago and is found in bacteria, plants, fungi, and animals. All members of this superfamily possess highly conserved regions of amino acid residues, and therefore there are

relatively small differences in the primary amino acid sequences of the CYPs across species. However, even small changes in the amino acid sequences can give rise to profound differences in substrate (and possibly effector) specificity and catalytic activity. Thus, differences in CYP isoforms between species are a major cause of species differences in drug metabolism (Table 1.2).

Table 1.2 CYP enzymes of the major drug-metabolizing CYP family in humans, rat, mouse, dog, and monkey [20].

Family	Subfamily	Human	Mouse	Rat	Dog	Monkey
CYP1	A	1A1, 1A2	1A1, 1A2	1A1, 1A2	1A1, 1A2	1A1, 1A2
	B	1B1	1B1	1B1	1B1	1B1
CYP2	A	2A6, 2A7, 2A13	2A4, 2A5, 2A12, 2A22	2A1, 2A2, 2A3	2A13, 2A25	2A23, 2A24
	B	2B6, 2B7	2B9, 2B10	2B1, 2B2, 2B3	2B11	2B17
	C	2C8, 2C9, 2C18, 2C19	2C29, 2C37, 2C38, 2C39, 2C40, 2C44, 2C50, 2C54, 2C55	2C6, 2C7[a], 2C11[a], 2C12[a], 2C13[a], 2C22, 2C23	2C21, 2C41	2C20, 2C43
	D	2D6, 2D7, 2D8	2D9, 2D10, 2D11, 2D12, 2D13, 2D22, 2D26, 2D34, 2D40	2D1, 2D2, 2D3, 2D4, 2D5, 2D18	2D15	2D17[b], 2D19[b], 2D29[b], 2D30[b]
	E	2E1	2E1	2E1	2E1	2E1
CYP3	A	3A4, 3A5, 3A7, 3A43	3A11, 3A13, 3A16, 3A25, 3A41, 3A44	3A1, 3A2[a], 3A9[a], 3A18[a], 3A23, 3A62	3A12, 3A26	3A8

a) Gender difference
b) Strain specific

1.4 General Compound Ionization Relationships

Compound ionization is the process of a neutral molecule (or atom) becoming a charged ion by gaining or losing electrons, often when a molecular compound is dissolved in water or through other chemical reactions. Drug molecules like acids or bases fully or partially ionize in aqueous environments by breaking their covalent bonds and forming separate ions. The reversible dissociation of a generic acid (HA) and generic base (B) in water (H_2O) is a split-off of a proton H^+ to form the conjugate base of the acid (A^-) and to form the conjugate acid of the base (BH^+), respectively (Figure 1.29).

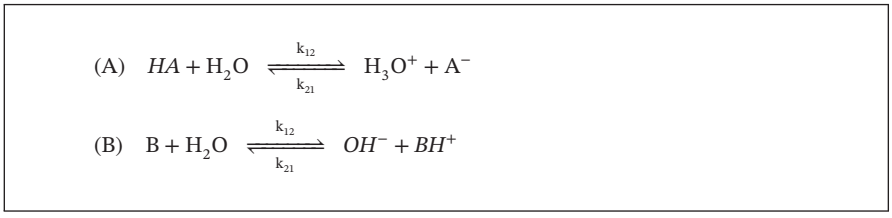


Figure 1.29 Reaction scheme for generic acid (panel A) and generic base (panel B) in water. The anion A^- is typically referred to as the conjugate base of acid HA, whereas the cation BH^+ is denoted as the conjugate acid of base B.

The (acid, base) equilibrium (dissociation) constants for these reactions are given by (compare Equation 1.33):

$$\text{Acid:} \quad K_{\text{HA}} = \frac{k_{21}}{k_{12}} = \frac{[\text{H}_3\text{O}^+] \cdot [A^-]}{[\text{HA}] \cdot [\text{H}_2\text{O}]} \tag{1.153}$$

$$\text{Base:} \quad K_{\text{B}} = \frac{k_{21}}{k_{12}} = \frac{[\text{BH}^+] \cdot [\text{OH}^-]}{[\text{B}] \cdot [\text{H}_2\text{O}]} \tag{1.154}$$

where k_{12} and k_{21} are the forward and backward reaction rate constants, respectively. As for aqueous solution, the concentration of water is constant (i.e., 55 mol/L). Consequently follows:

$$\text{Acid:} \quad K_a = K_{\text{HA}} \cdot [\text{H}_2\text{O}] = K_{\text{HA}} \cdot \text{const} = \frac{[\text{H}_3\text{O}^+] \cdot [\text{A}^-]}{[\text{HA}]} \tag{1.155}$$

$$\text{Base:} \quad K_b = K_{\text{B}} \cdot [\text{H}_2\text{O}] = K_{\text{B}} \cdot \text{const} = \frac{[\text{BH}^+] \cdot [\text{OH}^-]}{[\text{B}]} \tag{1.156}$$

where K_a and K_b are the so-called ionization constants which are indicators for the acid or the base strengths.

Definition of pH Value!

For a corresponding acid and base pair (remember – the conjugate base of the acid HA is A^-), knowing that in pure water at 25 °C the hydrogen ion (H_3O^+) and hydroxide ion (OH^-) concentrations are $1.0 \cdot 10^{-7}$ M, the relationship between K_a and K_b is as follows:

$$K_a \cdot K_b = \frac{[\text{H}_3\text{O}^+] \cdot [\text{A}^-]}{[\text{HA}]} \cdot \frac{[\text{HA}] \cdot [\text{OH}^-]}{[\text{A}^-]} = [\text{H}_3\text{O}^+] \cdot [\text{OH}^-]$$
$$= 1 \cdot 10^{-7} \frac{\text{mol}}{\text{L}} \cdot 1 \cdot 10^{-7} \frac{\text{mol}}{\text{L}} = 10^{-14} \left(\frac{\text{mol}}{\text{L}} \right)^2 = K_{aq} \tag{1.157}$$

where K_{aq} is the water equilibrium (dissociation) constant. pH and pOH are figures expressing the acidity or alkalinity of a solution on a logarithmic scale on which 7 is neutral. The "p" in the two terms refers to the negative logarithm

(pH and pOH are equal to −log10 c, where c is the H_3O^+ and OH− concentration in moles per liter, respectively).

Note!

pH is fundamentally a measure of hydronium ion (H_3O^+) concentration, which is often simplified to hydrogen ion (H^+) concentration. This is owned to the fact that, in aqueous solutions, between hydronium ions and hydrogen ions, a very fast equilibrium is established as follows – $H^+ + H_2O \rightleftharpoons H_3O^+$ (note – the term "fast equilibrium" highlights the dynamic nature of this process, where the ions are constantly forming and reacting but are always present in a balanced state). Hence, you will often see these terms used interchangeably.

Most of the time, the concentrations of these ions are very low or very large; thus, using pH makes it easier to work with such small or large values. Both scales run from 0 to 14. pH values lower than 7 are more acidic, while higher values are more alkaline, and for pOH values, the exact opposite applies, as illustrated in Figure 1.30.

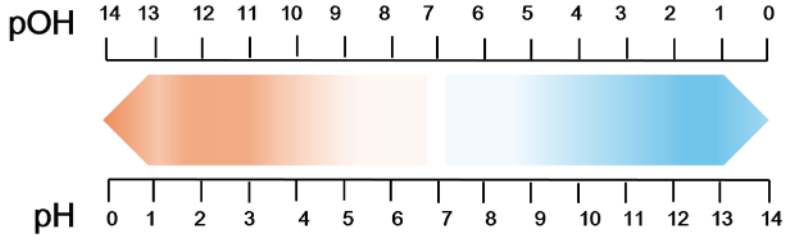


Figure 1.30 Comparison of pH and pOH scales of an aqueous solution. The brown zone refers to a more acidic environment (the brighter the more acidic) whereas the blue zone is indicative for an alkaline milieu (the brighter the more alkaline).

With the negative logarithms of K_a and K_b termed pK_a and pK_b, therefore follows (Appendix D):

$$\begin{aligned} pK_{aq} &= -\log K_{aq} = -\log(K_a \cdot K_b) = (-\log K_a) + (-\log K_b) \\ &= pK_a + pK_b = (-\log H_3O^+) + (-\log OH^-) \\ &= \mathrm{pH} + \mathrm{pOH} = 7 + 7 = 14 \end{aligned} \tag{1.158}$$

Equations 1.155 and 1.156 can be rearranged:

$$\text{Acid:} \quad \frac{1}{[H_3O^+]} = \frac{1}{K_a} \cdot \frac{[A^-]}{[HA]} \tag{1.159}$$

$$\text{Base:} \quad \frac{1}{[OH^-]} = \frac{1}{K_b} \cdot \frac{[BH^+]}{[B]} \tag{1.160}$$

Taking the negative log of Equations 1.159 and 1.160 we get, with reference to the relationships of Equations 1.157 and 1.158, the so-called Handerson–Hasselbach Equation:

$$\text{Acid:} \quad \text{pH} = pK_a + \log\frac{[A^-]}{[HA]} = pK_a - \log\frac{[HA]}{[A^-]} = 14 - pK_b + \log\frac{[A^-]}{[HA]} \tag{1.161}$$

Or:

$$\text{pOH} = pK_b + \log\frac{[A^-]}{[HA]} = 14 - pK_a + \log\frac{[A^-]}{[HA]} \tag{1.162}$$

$$\text{Base:} \quad \text{pOH} = pK_b + \log\frac{[BH^+]}{[B]} = 14 - pK_a + \log\frac{[BH^+]}{[B]} \tag{1.163}$$

Or:

$$\text{pH} = pK_a + \log\frac{[BH^+]}{[B]} = pK_a - \log\frac{[B]}{[BH^+]} = 14 - pK_b + \log\frac{[BH^+]}{[B]} \tag{1.164}$$

Buffer Solutions!

An aqueous solution consisting of a (tailored) mixture of a weak acid and its conjugate base (i.e., a salt derived from that acid) is called a buffer solution (or pH buffer or hydrogen ion (H^+) buffer). Buffer solutions are used as a means of keeping pH at a nearly constant value in a wide variety of chemical applications. Buffer solutions achieve their resistance to pH change because of the presence of an altered equilibrium between the weak acid HA and its conjugate base A^- in the reaction $HA \rightleftharpoons H^+ + A^-$ (compare Figure 1.29 (panel A)). When some strong acid is added to an equilibrium mixture of the weak acid and its conjugate base, hydrogen ions are added, and the equilibrium is shifted to the left in accordance with Le Châtelier's principle for the equilibrium reaction of the ionic association or dissociation (compare Section 3.2.3.2). Because of this, the hydrogen ion concentration increases by less than the amount expected for the quantity of strong acid added. Similarly, if strong alkali (base) is added to the mixture, the hydrogen ion concentration decreases by less than the amount expected for the quantity of alkali added because most of the added hydroxide ion (OH^-) is consumed in the reaction $OH^- + HA \rightarrow H_2O + A^-$ (compare Figure 1.29 (panel B)). The pH-value of buffer solutions changes relatively slowly in the buffer region, $\text{pH} = pK_a \pm 1$, where $[HA] \approx [A^-]$. Beyond this region, the pH alters rapidly though, as illustrated in Figure 1.31.

The so-called buffer capacity β quantifies the ability of a buffer solution to resist changes in pH by either absorbing or desorbing H+ and OH– ions. For monoprotic acid and its conjugate base, the relationship between buffer capacity and buffer concentrations is given by the Van Slyke Equation [21]:

$$\beta = \frac{n}{\Delta \mathrm{pH}} = 2.3 \cdot ([HA] + [A^-]) \cdot \frac{K_a \cdot [\mathrm{H_3O^+}]}{(K_a + [H_3O^+])^2}$$
$$= 2.3 \cdot ([HA] + [A^-]) \cdot \frac{K_a \cdot 10^{-\mathrm{pH}}}{(K_a + 10^{-\mathrm{pH}})^2} \tag{1.165}$$

where n is the number of moles of an acid or a base added per liter of buffer solution and ΔpH is the resulting change in pH.

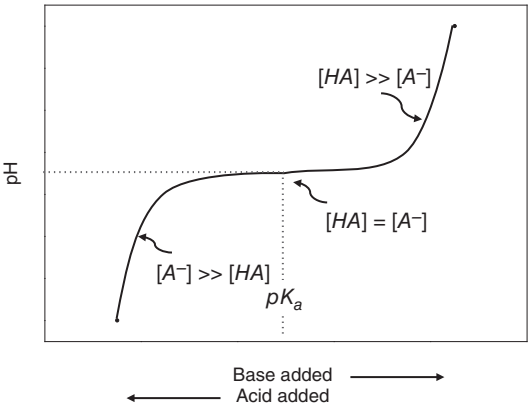


Figure 1.31 Change of pH of a buffer solution following addition of a strong base (e.g., NaOH) or a strong acid (e.g., HCl).

Based on Equations 1.161–1.164, the ionization term f_i - that is, the ionized fraction - can be expressed as the ratio of ionized to non-ionized molecular species, as follows:

$$\text{Acid:} \quad fi = \frac{[A^-]}{[HA]} = 10^{\mathrm{pH}-pKa} = \frac{1}{10^{pK_a - \mathrm{pH}}} \tag{1.166}$$

$$\text{Base:} \quad fi = \frac{[BH^+]}{[B]} = 10^{pKa-\mathrm{pH}} = \frac{1}{10^{\mathrm{pH}-pKa}} \tag{1.167}$$

By definition, the ionization term for neutral (non-ionizable) compounds is zero (i.e., $fi = 0$). Graphically, the relationships according to Equations 1.166 and 1.167 can be illustrated as shown in Figure 1.32:

Hence, the fraction of drug not ionized (*fui*) is represented by:

$$\text{Acid:} \quad fui = \frac{[HA]}{[A^-]} = 1 - fi = \frac{[HA]}{[A^-] + [HA]} = \frac{1}{1 + \frac{[A^-]}{[HA]}}$$
$$= \frac{1}{1 + 10^{\mathrm{pH}-pKa}} = \frac{1}{1 + \frac{1}{10^{pKa-\mathrm{pH}}}} = \frac{10^{pKa-\mathrm{pH}}}{1 + 10^{pKa-\mathrm{pH}}} \tag{1.168}$$

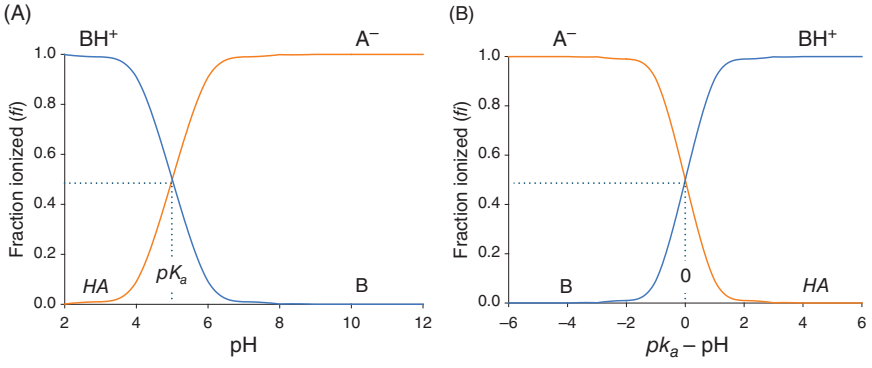


Figure 1.32 Change of the degree of ionization as a function of pH (panel A) and pK_a – pH (panel B) for monoprotic acids (orange line) and bases (blue line) according to Equation 2.31 (*k*/*l*) demonstrating that the percentage ionized at pHs greater and lower than ~2 units the pK_a are <1% and > 99%, respectively. Example refers to a pK_a-value of 5.

$$\text{Base:}\quad fui = \frac{[B]}{[BH^+]} = 1 - fi = \frac{[B]}{[BH^+]+[B]} = \frac{1}{1+\frac{[BH^+]}{[B]}}$$
$$= \frac{1}{1+10^{pKa-\text{pH}}} = \frac{1}{1+\frac{1}{10^{\text{pH}-pKa}}} = \frac{10^{\text{pH}-pKa}}{1+10^{\text{pH}-pKa}} \qquad (1.169)$$

Calculation of Unionized Fractions in the Blood and Tissues!

The pH values of blood and intracellular tissue water are typically assumed to be 7.4 and 7.0–7.1, respectively. Consequently, referring to Equations 1.168 and 1.169, the fui ratio between plasma (p) and tissues (tis) (i.e., $fui_p/fui_{tis} = fui_{7.4}/fui_{7.1}$) becomes < 1 or > 1 for acids and bases, respectively.

For multiprotic compounds (containing a number > 1 of possible positively- or negatively-charged functional groups) and zwitterions (containing an equal number

Table 1.3 Assessment of unionized fractions of monoprotic vs. diprotic compounds

	Monoprotic[a)]	Diprotic[b), c)]	
	$fui = X/(1+X)$	$fui = X/(1+X)\cdot Y/(1+Y)$	
Acids	$X = 10^{pka-\text{pH}}$	$X = 10^{\text{pka1}-\text{pH}}$	$Y = 10^{\text{pka2}-\text{pH}}$
Bases	$X = 10^{\text{pH}-\text{pKa}}$	$X = 10^{\text{pH}-\text{pKa1}}$	$Y = 10^{\text{pH}-\text{pKa2}}$
Zwitterions[d)]	—	$X = 10^{\text{pka(acid)}-\text{pH}}$	$Y = 10^{\text{pH}-\text{pKa(base)}}$

a) Number of functional groups charged is 1
b) Number of functional groups charged is 2
c) $pK_{a1} < pK_{a2}$
d) Contain one acidic and one basic group

of possible positively- and negatively-charged functional groups, also known as inner salts or dipolar ions), the *fi* (or *fui*) relationships are becoming increasingly complex as summarized and exemplified in Table 1.3 [22, 23].

References

1 Available from: https://en.wikipedia.org
2 Kwon, Y. (2013). *Handbook of Essential Pharmacokinetics, Pharmacodynamics, and Drug Metabolism for Industrial Scientists*. Springer US.
3 Lee, Z. (2022). Mathematical model and its classifications. *RRJSMS* 8: 9–10.
4 Marion, G. (2008). An introduction to mathematical modelling. In: *Bioinformatics and Statistics*. Scotland: University of Bristol.
5 Copeland, R. (2004). *Enzymes: A practical introduction to structure, mechanism, and data analysis*, 2e. John Wiley & Sons.
6 Bisswanger, H. (2017). *Enzyme Kinetics: Principles and Methods*. Wiley-VCH.
7 Eigen, M. (1963). Protonenuebertragung, Saure-Base-Katalyse und enzymatische Hydrolyse. *Angew. Chem.* 12: 489–588.
8 Murdoch, J. (1972). Rate-equilibriums relations and proton-transfer reactions. *J. Am. Chem. Soc.* 94: 4410–4418.
9 Camenisch, G., Folkers, G., and van de Waterbeemd, H. (1996). Review of theoretical passive drug absorption models: historical background, recent developments and limitations. *Pharm. Acta Helv.* 71: 309–327.
10 Buchwald, P. and Bodor, N. (2001). A simple, predictive, structure-based skin permeability model. *JPP* 53: 1087–1089.
11 Silbey, R. and Alberty, R. (2001). *In Physical Chemistry*, 3e. John Wiley & Sons New York.
12 Evans, W. and Relling, M. (1999). Pharmacogenomics: translating functional genomics into rational therapeutics. *Science* 286: 487–491.
13 Chauret, N., Gauthier, A., and Nicoll-Griffith, A. (1998). Effect of common organic solvents on in vitro cytrochrome P450-mediated metabolic activities in human liver microsomes. *Drug Metab. Dispos.* 26 (1): 1–4.
14 Schiller, H., Camenisch, G., and Huth, F. (2023). Introduction to fundamentals of drug-drug interactions. In: *Current Topics in Non-Clinical drug Development*, vol. 2 (ed. A. Li), 332–371. CRC Press.
15 Cha, S. (1968). Kinetics of enzyme reactions with competing alternative substrates. *Mol. Pharmacol.* 4: 621–629.
16 Pocklington, T. and Jeffery, J. (1969). Competition of two substrates for a single enzyme: a simple kinetic theorem exemplified by a hydroxy steroid dehydrogenase reaction. *Biochem. J.* 112: 331–334.
17 Cornish-Bowden, A. (1995). *Fundamentals of Enzyme Kinetics*, 2e. Portland Press London.
18 Korzekwa, K., Krishnamachary, N., Shou, M. et al. (1998). Evaluation of atypical cytochrome P450 kinetics with two-substrate models: evidence that multiple

substrates can simultaneously bind to cytochrome P450 active sites. *Biochemistry* 36: 4137–4147.

19 Tracy, T. (2003). Atypical enzyme kinetics: their effect on in vitro-in vivo pharmacokinetic predictions and drug interactions. *Curr. Drug Metab.* 4: 341–346.

20 Martignoni, M., Groothuis, G., and de Kanter, R. (2006). Species differences between mouse, rat, dog, monkey and human CYP-mediated drug metabolism, inhibition and induction. *Expert Opin. Drug Metab. Toxicol.* 2: 875–894.

21 Urbansky, E. and Schock, M. (2000). Understanding, deriving, and computing buffer capacity. *J. Chem. Educ.* 77: 1640–1644.

22 Rodgers, T. and Rowland, M. (2007). Mechanistic approaches to volume of distribution predictions: understanding the processes. *Pharm. Res.* 24: 918–933.

23 Berry, L., Roberts, J., Be, X. et al. (2010). Prediction of V(ss) from in vitro tissue-binding studies. *Drug Metab. Dispos.* 38: 115–121.